PHOTOCATALYTIC REDUCTION OF CARBON DIOXIDE TO METHANE OVER NIO/TIO_2 IN GAS PHASE UNDER UV LIGHT ILLUMINATION

[1]PEI-CHEN LEE, [2]YOUNG KU, [3]GIANG LUONG

National Taiwan University of Science and Technology
E-mail: [1]ty77op@gmail.com, [2]ku508@mail.ntust.edu.tw, [3]luong.kimgiang07@gmail.com

Abstract - Pure TiO_2 photocatalyst doped with nickel oxide (NiO/TiO_2) was synthesized by impregnation method and coated on glass substrates used for reducing carbon dioxide in gas phase. The photocatalytic reduction of CO_2 was conducted in a planar reactor under UV illumination with a light intensity of 25.34 $mWcm^{-2}$in 90 min. The characterization of photocatalysts was observed by XRD, SEM, N_2 adsorption–desorption, UV–vis. The effects of CO_2 initial concentration, the relative humidity and the amount of NiO loading on the photoreduction process was investigated. The product, CH_4 were formed in order: 10 wt% NiO/TiO_2 > TiO_2 > 20 wt% NiO/TiO_2. In this study, the highest yield of CH_4 was 401 $ppm/g_{catalyst}$ in the optimal operation condition: 600 ppm initial concentration, 45 % relative humidity using 10 wt% NiO/TiO_2.

Index terms - Nio, Photocatalysis, P-N Junction, Tio_2

I. INTRODUCTION

Carbon dioxide (CO_2) is the largest source of greenhouse gas, which plays a significant role in resulting in the global climate change and pollution environment, motivating scientists to reduce CO_2 emission [1], [2]. Carbon dioxide obtained after capturing is used to make new materials and fuels such as methanol (CH_3OH), methane (CH_4), carbon monoxide (CO), and formic acid (HCOOH). However, carbon dioxide is a chemically stable compound with carbon-oxygen bond so its conversion requires substantial energy input [3], [4]. Carbon dioxide photocatalysis over semiconductor under light irradiation is the potential to solve this problem because it can not only reduce CO_2 level but also produce fuel without any secondary pollutants. Among the various semiconducting materials, titanium dioxide (TiO_2) photocatalyst is the most suitable because of its high chemical stability, nontoxic nature, low cost, and easy availability [5]. Generally, the photoreduction of carbon dioxide in gas phase comprises two steps: CO_2 adsorption and CO_2-to-hydrocarbon conversion. Firstly, carbon dioxide molecules adsorb on the photocatalyst surface. And then, the photogenerated electrons migrate from the bulk to the surface to reduce CO_2 to CH_4. Nevertheless, in the second step, a large proportion of photogenerated electrons combine with the holes in the bulk and cannot migrate tothe surface to take part in the photocatalytic reaction, leading to a poor photocatalytic activity [6].

Therefore, it is necessary to modify TiO_2 catalyst to enhance the CO_2 adsorption on catalyst product yield rates of this process [7]. Many methods have been used to effectively promote the photogenerated electron–hole recombination probability. Fabrication of photocatalysts heterojunction is one of the methods which can induce faster carrier migration. Despite the wide band gap, nickel oxide (NiO) is p-type semiconductor, which can form p-n heterojunction with TiO_2 (n-type semiconductor). The p-n heterojunction can reduce the recombination of photogenerated electrons and holes, which is beneficial for photocatalytic activity and photoelectrochemical performance of materials [8], [9]. In this study, we focus on improving the photocatalytic capacity of TiO_2 by doping with NiO, establishing the optimal condition for the photoreduction of CO_2 in gas phase.

II. EXPERIMENTALS

A. The preparation of NiO/TiO_2 photocatalyst coated glass substrates

$NiO-TiO_2$ films were prepared on glass substrates by impregnation method. Glass substrates were pretreated by cleaning with distilled water, ethanol, and acetone for 30 min, then rinsing and drying in the oven at 120 ^{0}C for 1 h. At room temperature, 1 g P25 powder was mixed into a solution of nickel nitrate hexahydrate ($Ni(NO_3)_2.6H_2O$), isopropyl alcohol (IPA – with liquid/solid ratio was 10 wt%). Ethanol (C_2H_5OH) also was added into this solution with IPA/ethanol ratio was 3 wt% and stirred continuously for 30 min. The weight percentage of nickel oxide (NiO) in the photocatalyst was 0, 10 and 20 wt%. The pretreated glass substrate was dipped into the receive precursor for 3 min and lifted out slowly. The glass substrate obtained was then dried at 120 ^{o}C for 4 min followed by calcination in air at 400 ^{o}C for 2 h. The pure TiO_2 was prepared via the same route with a mixture of 1 g P25 and 2 ml ethanol.

B. Characterization

The X-ray diffraction (XRD) measurement is used to determine the chemical composition and crystal structure of photocatalysts, using Bruker

diffractometer (D2 PHASER) with Cu K□ radiation at room temperature in the range of 2□ from 20° to 80°. This process was operated at 40 kV, 40 mA with a sampling interval of 0.05^0 and scan speed 0.5°/minute. The average grain size of the products was calculated from full-width at half maxima (FWHM) of corresponding X-ray diffraction peaks by Scherrer's formula. The Brunauer-Emmett-Teller (BET) specific surface of photocatalysts was calculated from the nitrogen adsorption–desorption isotherms by a Quantachrome Autosorb-1 analyzer at 77 K. Prior to the gas adsorption measurement, a proximately 0.2 g of NiO/TiO_2 photocatalyst was degassed at 150 ^{0}C under vacuum condition for 5 h. Field Emission Scanning Electron Microscope (FE-SEM) and energy dispersive spectroscopy (EDS) were conducted on JEOL JSM-7900F under a working voltage of 15kV and the pressure in the chamber was kept below 4.41 x 10^{-4} Pa. The optical properties as energy bandgap of photocatalysts were obtained from UV-vis Diffuse Reflectance Spectra (UV-DRS) with the wavelength range of 200-800 nm.

C. Photocatalytic CO_2 reduction

The photocatalytic reduction of CO_2 in gas phase was performed in the continuous-flow mode in a two-parallel-plate reactor with of 0.38 width and 0.1 m length (Fig. 1). A hollow fillister of 0.30 m length, 0.05 m wide, and 0.15 m depth was contained at the bottom fixture as the flow channel, with the effective volume of the planar photoreactor was 225 ml.

The photocatalyst-coated on glass substrates were assembled at the bottom of the reactor. UV illumination was carried out by Hg lamp with an intensity of 25.34 mWcm^{-2}, which was from the top of the planar reactor. The gas products were analyzed using a gas chromatograph (GC) Agilent 7890A equipped with Thermal Conductivity Detector (TCD).

III. RESULTS AND DISCUSSION

A. Characterization of Photocatalysts

The crystal phase of all samples calcined at 400 ^{0}C are shown in Fig. 2. Anatase was the major phase in the structure of commercial P25 with the main peak at 2θ= 25.2^0, 38.0^0, 48.2^0, 54.3^0 and 62.2^0. Rutile-TiO_2 exhibits characteristic diffraction pattern at 2θ = 27.2^0, 35.6^0, 38.8^0, 40.7^0 and 53.6^0. XRD patterns indicatde the existence of both the anatase (A) and the rutile (R) phase structure of TiO_2 (JCPDS, no. 01-071-1169; JCPDS, no. 01-076-0323) [10].

Table I

Photocatalyst	TiO_2	10 wt% NiO/TiO_2	20 wt% NiO/TiO_2
Specific surface area m^2/g	58.374	58.842	56.814
Total pore volume cm^3/g	13.412	13.519	13.053

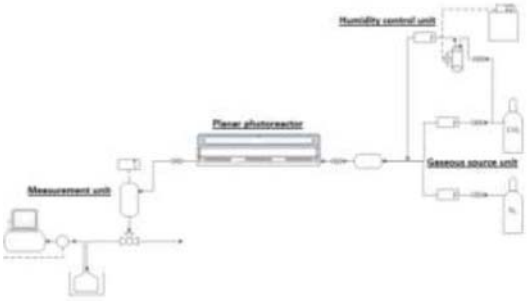


Fig. 1. Scheme diagram of photocatalytic reduction of carbon dioxide in gas phase.

The XRD pattern of NiO doped TiO_2 showed the peak of NiO (JCPDS, no. 01-073-1519) is similar to the peak of anatase-TiO_2 expect for the peak in 43^0. Depending on the weight ratio of Ni/Ti, the intensity of the peak of 20wt % NiO/TiO_2 was higher than the intensity of the peak of 10wt% NiO/TiO_2. Furthermore, there were no peaks of other mixed oxides, which indicated that only NiO/TiO_2 composites were formed.

Table I shows a slight change in surface area and total pore volume of these photocatalysts. The specific area surface of TiO_2 was similar to 10 wt% NiO/TiO_2, as 58.374 and 58.842 m^2/g, respectively. However, a decrease was observed in 20 wt% NiO/TiO_2, 56.814 m^2/g. The total pore volume of catalyst also decreased with increasing the Ni loading. It has been explained that NiO contributed to the blockage of mesopores on the surface of photocatalyst [11].

SEM photographs of TiO_2 and 10 wt% NiO/TiO_2 and 20 wt% NiO/TiO_2 are exhibited in Fig. 3. The nanostructures of TiO_2 were dense with high agglomeration in Fig. 3 (a). The SEM images of nanostructure of NiO/TiO_2 in Fig. 3 (b) and (c) show the similar in morphology, which observed as the porous structure. This type of structure was formed by the agglomeration of nanoparticles, which consisted of the NiO/TiO_2 heterojunction material.

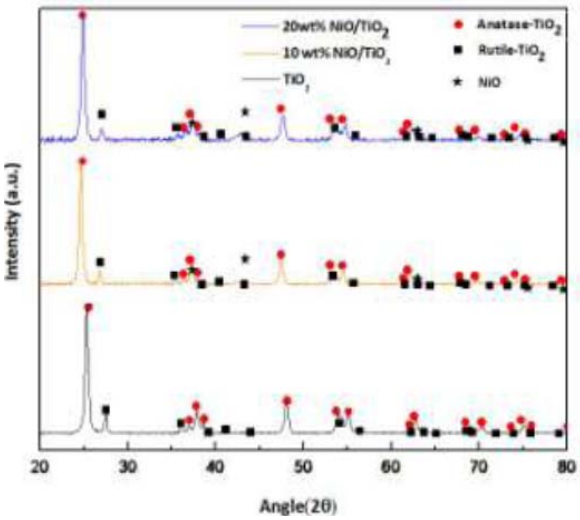


Fig. 2. Xrd patterns of prepared photocatalysts.

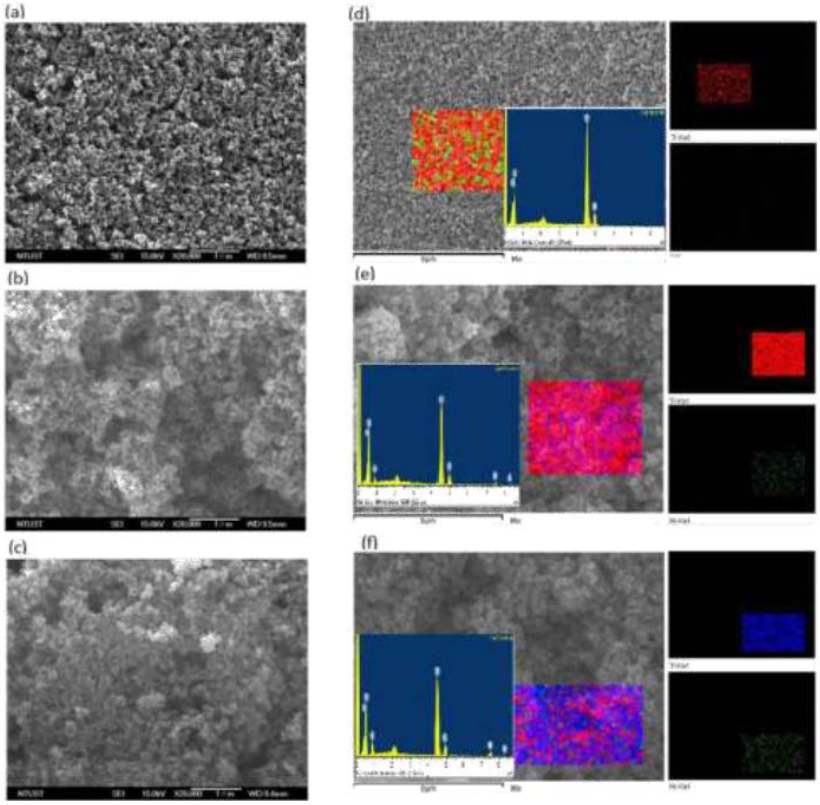


Fig. 3. SEM images and EDS elemental mapping analysis of (a, d) TiO_2, (b, e) 10wt% NiO/TiO_2, (c, f) 20wt% NiO/TiO_2.

UV-vis diffuse reflectance spectra (UV-vis DRS) of these prepared photocatalysts are shown in Fig. 4. The absorbance edge was gradually red-shifted with the increase of NiO loading. This result also demonstrates that NiO/TiO_2 can absorb not only the ultraviolet light but also visible light. The same results have been found in previous research [12]. The band gap energy was calculated by Tauc equation:

$$(\alpha h\nu)^{1/n} = A(h\nu - E_g) \quad (1)$$

where α, h, ν, A, Eg are absorption coefficient, planck constant, frequency, proportionality constant, band gap energy, respectively. n = 1/2 for the direct band. Plotting $(\alpha h\nu)^2$ verse hν from the absorption spectra and extrapolating the line to zero on an X-axis, from the intersections of the straight lines obtained can present the optical band gap energy. As can be seen, a decrease in band gap was observed when increasing the NiO loading. The result shows TiO_2 on glass substrates loading with 0, 10 and 20 wt% NiO deduced the bandgaps of 3.20, 3.15 and 3.04 eV, respectively. This narrowing trend of bandgap can be explained by the high dispersion of nickel particles on the surface of TiO_2, which caused the plasmon resonance [13].

B. Photoctalytic Reduction of Carbon Dioxide

Fig. 5 shows the effect of initial carbon dioxide concentration, which was set to 200, 600, 800, 1100 and 1400 ppm on the photocatalytic reduction in various loading of NiO. The amount of product increased gradually in the 30 first minutes of reaction and became stable after reaching the maximum amount. A decreasing trend of yield was found at each concentration using 20 wt% NiO/TiO_2. Partially, at the initial 600 ppm CO_2, the highest formation of CH_4 was reached 94, 127 and 66 ppm/$g_{catalyst}$ using 0, 10 and 20 wt% NiO/TiO_2, respectively.

A decrease in the CH_4 was found when increasing the inlet carbon dioxide concentration higher than 600 ppm. It can be explained that exceed CO_2 concentration results in the more adsorbed molecules and saturation of the active sites. Therefore, the photocatalytic reduction of CO_2 was limited significantly [14].

Table II Element content of the prepared samples.

Samples	EDS elemental composition (wt%)		
	Ti	O	Ni
TiO_2	55.23	44.77	0
10 wt% NiO/TiO_2	46.77	48.32	4.91
20 wt% NiO/TiO_2	45.49	44.69	9.82

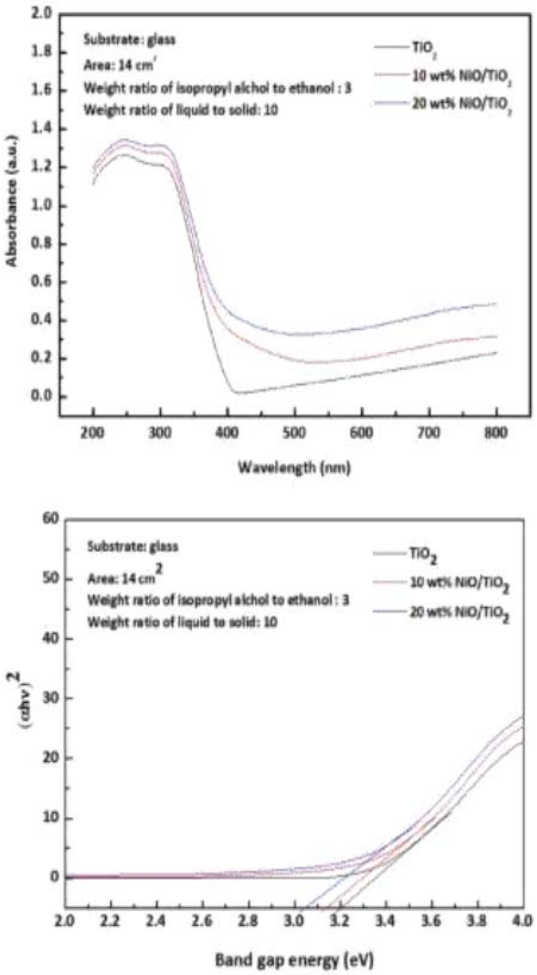


Fig. 4. Tauc plots of NiO/TiO_2 on glass substrates doping with different weight percent of NiO.

The relative humidity plays an important role in the reduction of CO_2. The water molecules can react with the hole and generate some hydroxyl groups, which enhance the photoreduction. On the other hand, the presence of H_2O can bring negative impacts [15]. Therefore, this study conducts an experiment to investigate the impact of H_2O at the optimal initial CO_2 concentration of 600 ppm without any change in operating conditions. Fig. 6 shows the formation of CH_4 in various relative humidity 10, 45, and 85 with all prepared photocatalysts.

The photoreduction of CO_2 produced the highest CH_4 when the relative humidity was 45, about 158, 401 and 98 ppm/$g_{catalyst}$ using 0, 10 and 20 wt% NiO/TiO_2 respectively. When the relative humidity was higher than 45 %, the formation of CH_4 decreased dramatically. In partially, CH_4 yield reduced from 150 ppm/ $g_{catalyst}$ to 20 ppm/ $g_{catalyst}$ with the range in 45 % and 85 % of humidity using pure TiO_2. Huang indicates that the more water molecules, excess water can compete with CO_2 by occupying the active site on the surface of TiO_2 [16]. Furthermore, absorbed CO_2 can be replaced by H_2O because the binding energy of H_2O is higher than of CO_2 on the surface of TiO_2 [17].

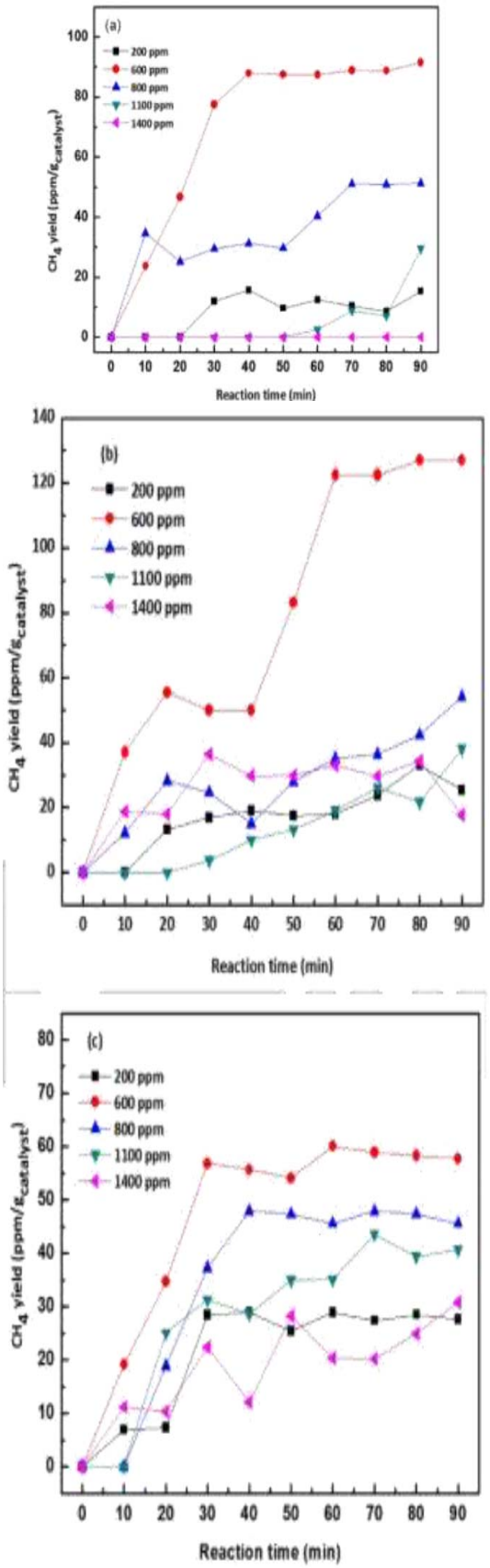


Fig. 5. The CH_4 yield of photocatalytic reduction various initial CO_2 concentration in (a) TiO_2, (b) 10 wt% NiO/TiO_2 and (c) 20 wt% NiO/TiO_2.
(Condition: flow rate 150 ml/min, light intensity 25.43 mW/cm^2, relative humidity (RH) 10%)

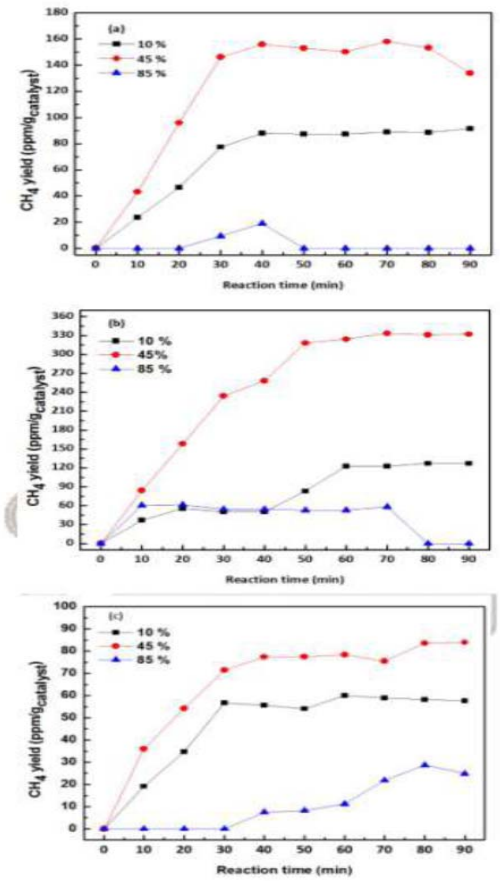


Fig. 6. The CH_4 yield of photocatalytic reduction various relative humidity in (a) TiO_2, (b) 10 wt% NiO/TiO_2 and (c) 20 wt% NiO/TiO_2.
(Condition: flow rate 150 ml/min, light intensity 25.43 mW/cm^2, initial CO_2 concentration 600 ppm)

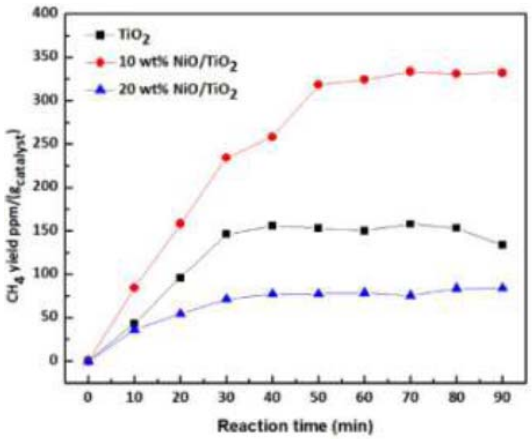


Fig. 7. The yield of CH_4 over various NiO loading on TiO_2. (Condition: flow rate 150 ml/min, light intensity 25.43 mW/cm^2 , initial CO_2 concentration 600 ppm, relative humidity: 45 %)

In the optimal condition 600 ppm CO_2 and 45 % relative humidity, the formation of CH_4 was reached the highest value in the order: 10 wt% NiO/TiO_2 > TiO_2 > 20 wt% NiO/TiO_2, with the optimal loading of NiO was 10 wt% as Fig.7. Doping NiO provides the active reaction sites, thus it enhances the photocatalytic activity of TiO_2 [18]. However, in the high amount of NiO (20 wt% NiO/TiO_2), a decrease of photocatalytic reduction was observed. Chen indicates that increasing of NiO results in reducing of illumination area of TiO_2 [8]. In addition, the decrease of the specific surface area of 20 wt% NiO/TiO_2 can be explained for the negative impact of high loading of NiO.

REFERENCES

[1] H. R. Kim, A. Razzaq, C. A. Grimes, and S.-I. In, "Heterojunction p-n-p $Cu_2O/S-TiO_2/CuO$: Synthesis and application to photocatalytic conversion of CO_2 to methane," Journal of CO_2 Utilization, vol. 20, pp. 91-96, July 2017.

[2] H. Y. Lee, A. R. Kim, M.-J. Park, J. M. Jo, D. H. Lee, and J. W.

[3] Bae, "Combined steam and CO_2 reforming of CH_4 using coke oven gas on nickel-based catalyst: Effects of organic acids to nickel dispersion and activity," Chemical Engineering Journal, vol. 280, pp. 771-781, November 2015.

[4] O. Ola, and M. M. Maroto-Valer, "Review of material design and reactor engineering on TiO_2 photocatalysis for CO_2 reduction," Journal of Photochemistry and Photobiology C: Photochemistry Reviews, vol. 24, pp. 16-42, September 2015.

[5] L. Yuan, and Y.-J. Xu, "Photocatalytic conversion of CO_2 into value-added and renewable fuels," Applied Surface Science, vol. 342, pp. 154-167, July 2015.

[6] K. Li, B. Peng, and T. Peng, "Recent Advances in heterogeneous photocatalytic CO_2 conversion to solar fuels," ACS Catalysis, vol. 6, no. 11, pp. 7485-7527, November 2016.

[7] X. Chang, T. Wang, and J. Gong, "CO_2 photo-reduction: insights into CO_2 activation and reaction on surfaces of photocatalysts," Energy & Environmental Science, vol. 9, no. 7, pp. 2177-2196, 2016.

[8] B. a. T. Tahir, Muhammad and Saidina Amin, Nor Aishah, "Photocatalytic carbon dioxide and methane reduction to fuels over La-promoted titanium dioxide nanocatalyst," Chemical Engineering Transactions, vol. 56, April 2017.

[9] C.-J. Chen, C.-H. Liao, K.-C. Hsu, Y.-T. Wu, and J. C. S. Wu, "P–N junction mechanism on improved NiO/TiO_2 photocatalyst," Catalysis Communications, vol. 12, no. 14, pp.1307-1310, August 2011.

[10] J. H. Lee, S.-I. Kim, S.-M. Park, and M. Kang, "A p-n heterojunction NiS-sensitized TiO_2 photocatalytic system for efficient photoreduction of carbon dioxide to methane," Ceramics International, vol. 43, no. 2, pp. 1768-1774, February 2017.

[11] S. R. Shirsath, D. V. Pinjari, P. R. Gogate, S. H. Sonawane, and A. B. Pandit, "Ultrasound assisted synthesis of doped TiO_2 nano-particles: characterization and comparison of effectiveness for photocatalytic oxidation of dyestuff effluent," Ultrason Sonochem, vol. 20, no. 1, pp. 277-86, Jan 2013.

[12] Y. Lv, Z. Xin, X. Meng, M. Tao, and Z. Bian, "Ni based catalyst supported on KIT-6 silica for CO methanation: Confinement effect of three dimensional channel on NiO and Ni particles,"

[13] Microporous and Mesoporous Materials, vol. 262, pp. 89-97, 2018.

[14] B. Gao, T. Wang, X. Fan, H. Gong, H. Guo, W. Xia, Y. Feng, X.

[15] Huang, and J. He, "Synthesis of yellow mesoporous Ni-doped TiO_2 with enhanced photoelectrochemical performance under visible light," Inorganic Chemistry Frontiers, vol. 4, no. 5, pp. 898-906, 2017.

[16] O. Ola, and M. Mercedes Maroto-Valer, "Role of catalyst carriers in CO_2 photoreduction over nanocrystalline nickel loaded TiO2-based photocatalysts," Journal of Catalysis, vol. 309, pp. 300-308, 2014.

[17] M. Dilla, R. Schlögl, and J. Strunk, "Photocatalytic CO_2 reduction under continuous flow high-purity conditions: quantitative evaluation of CH_4 formation in the steady-state," ChemCatChem, vol. 9, no. 4, pp. 696-704, 2017.

[18] Z. Huang, X. Cheng, P. Dong, and X. Zhang, "Effect of electric field on CO_2 photoreduction by TiO_2 film," Journal of Electronic Materials, vol. 46, no. 2, pp. 999-1004, 2016.
[19] M. D. A. M. S. R. J. Strunk, "Photocatalytic CO_2 reduction
[20] under continuous flow high-purity conditions: influence of light intensity and H_2O concentration," ChemCatChem, vol. 9, no. 23, pp. 4343-4352, December 2017.
[21] K. Li, X. An, K. H. Park, M. Khraisheh, and J. Tang, "A critical review of CO_2 photoconversion: Catalysts and reactors," Catalysis Today, vol. 224, pp. 3-12, April 2014.
[22] A. Sharma, and B.-K. Lee, "Photocatalytic reduction of carbon dioxide to methanol using nickel-loaded TiO_2 supported on activated carbon fiber," Catalysis Today, vol. 298, pp. 158-167, December 2017.

★★★